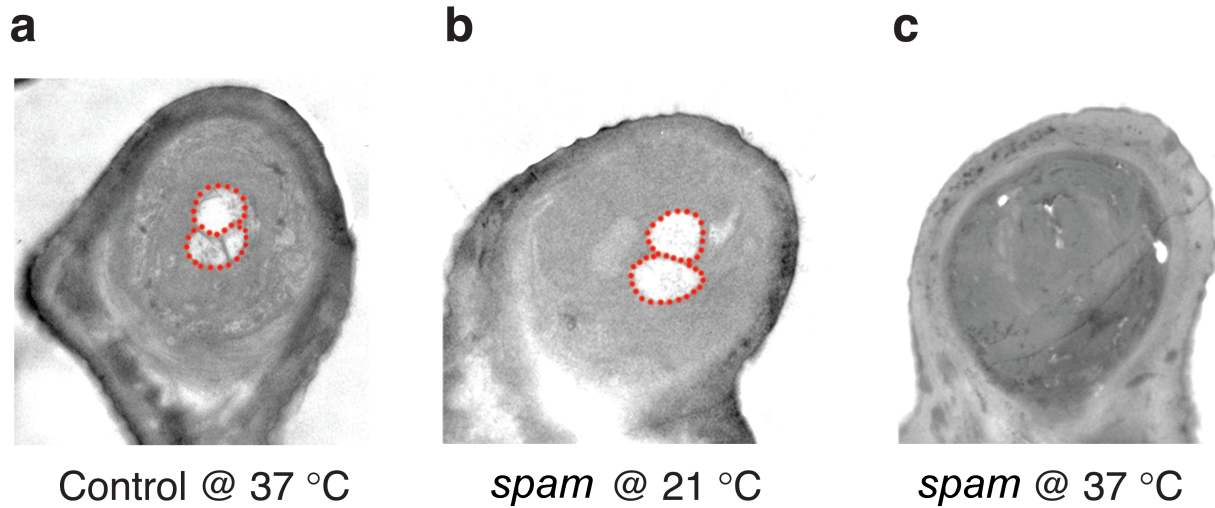
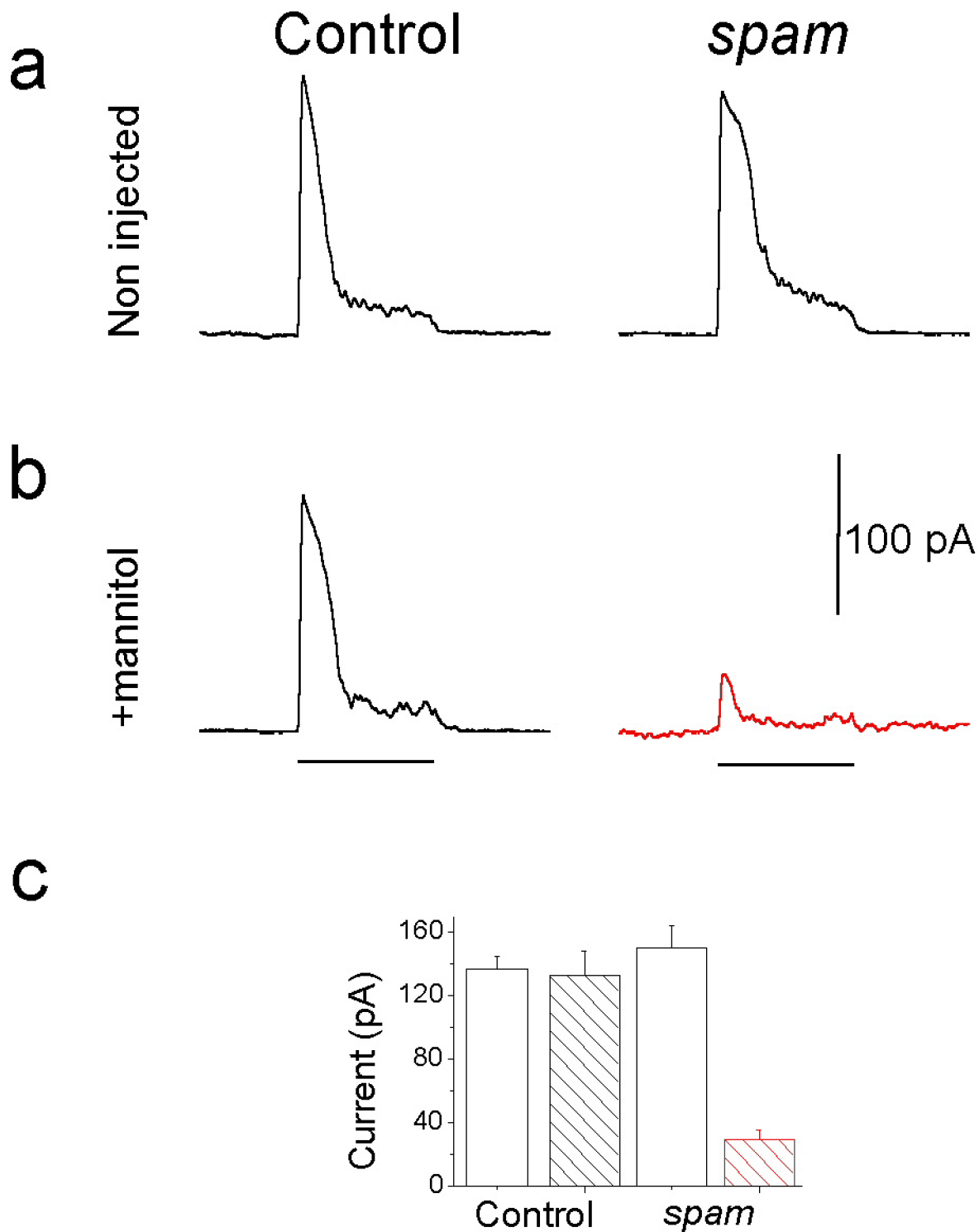


**Supplementary Figure 1: Behavioral phenotype of *spam* flies.** Control (*cn bw*) and *spam* flies were placed at 37°C and examined every 15min for their ability to stand upright or to walk. Error bars indicate standard deviation; n=5 dishes with 10 flies each. The uncoordination phenotype is cannot be reversed, even after returning the flies to low temperature conditions.

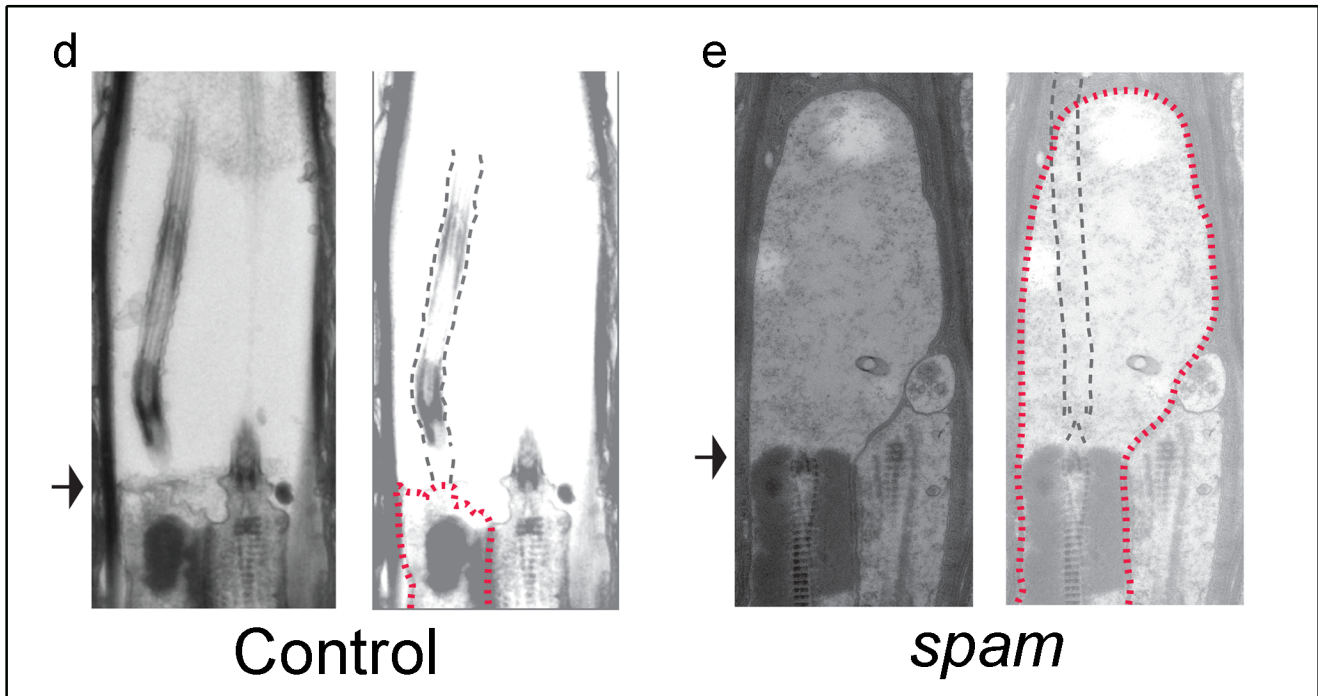
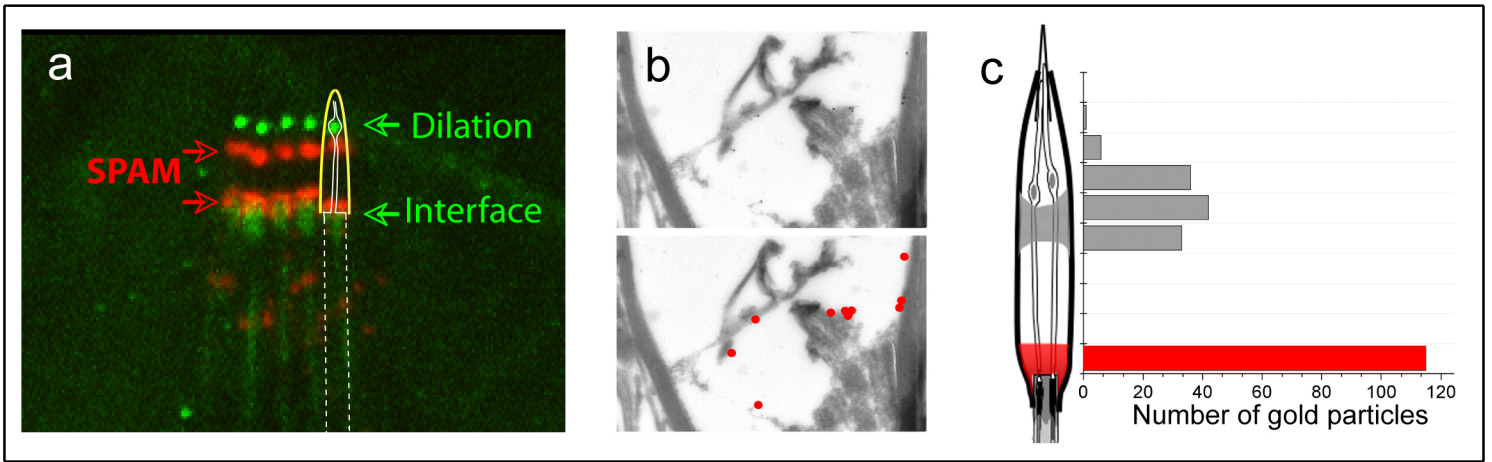


**Supplementary Figure 2: Heat exposure causes chemoreceptors of *spam* mutants to undergo dramatic cellular deformation.** In addition to MRNs, Spam is also expressed in chemosensory neurons. Shown are typical electron micrographs of cross sections through the base of a chemosensory bristle. **(a)** control *cn bw* flies at 37°C and **(b)** *spam* mutants at 21°C have nearly indistinguishable morphology. However, **(c)** heat treatment of *spam* flies results in the collapse and near total loss of the chemoreceptor outer segments (delineated by the red dotted lines). Shown are 150 nm thick sections at the tip of the 3<sup>rd</sup> antennal segment, at the point where the bristle connects with the cuticle. Tissue preparation and electron microscopy were performed as described previously<sup>7</sup>.



**Supplementary Figure 3: Spm MRNs are sensitive to osmotic shock**

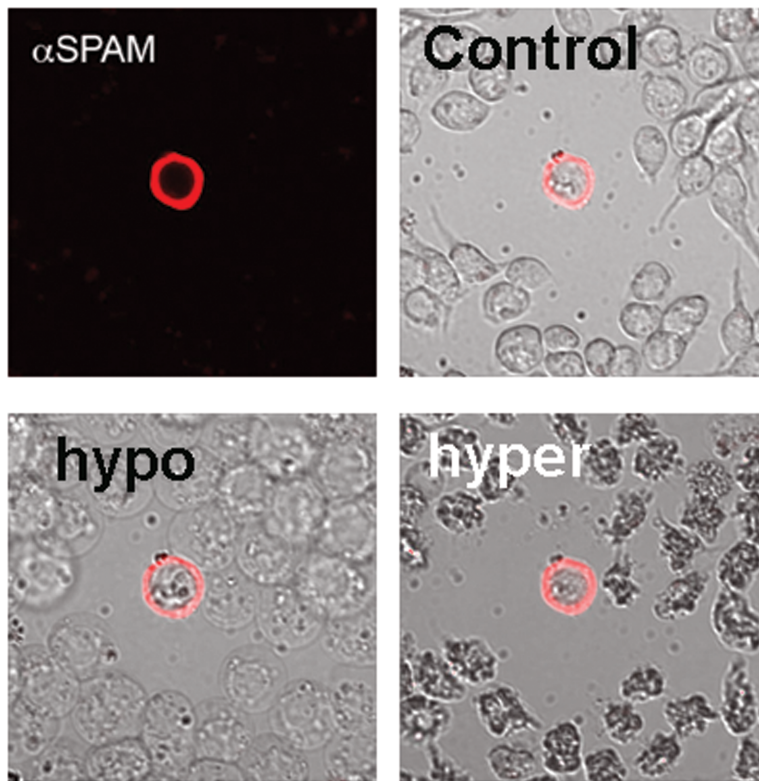
**a-b**, MRN responses from a single voltage-clamped bristle to mechanical stimuli. Upper panel (left to right): responses of untreated control (*cn bw* flies) and *spam* (*spam/spam* mutants). **b**, After injection of 1 M mannitol and incubation for 15 minutes at 21°C (lower panel), responses were abolished in *spam* mutants (red trace), but not in control animals. Lines under the traces indicate the 0.3 sec. duration of a 30 $\mu$ m deflection stimuli. **c**, Summary of peak responses of **a-b**. Error bars indicate standard deviation (n=5 for each trial).



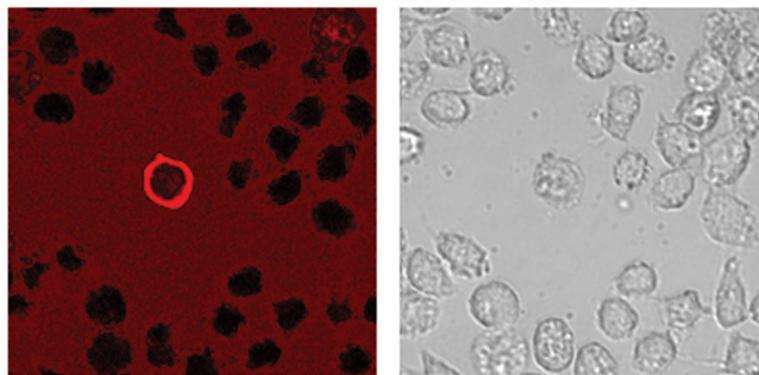
**Supplementary Figure 4: Spam is localized at the interface between the MRN and the lymph space.**

(a) Confocal image of larval *lc5* chordotonal mechanoreceptor neurons expressing an outer-segment GFP reporter (*Oseg4*) that marks both the interface between the base of the cilia and the lymph space, and the ciliary dilation region (green)<sup>19</sup>. The tissue was also labeled with *mab21A6* anti-Spam antibodies to mark the location of Spam protein (red). The superimposed scolopale diagram and dotted lines highlight one of the five chordotonal neurons in the image. (b) Immunogold electron microscopy on frozen sections of the Johnston's organ. Shown are electron micrographs of a single scolopale immunolabeled with anti-Spam antibodies and 10 nm gold particles. The panels are from the interface between the MRN and the lymph space, at the base of the cilium. The bottom panel shows the gold particles in pseudocolor (red). (c) Gold particle count along the scolopale length, starting at the interface between the MRN and the lymph space (labeled in red) and ending at the cap; the entire organ was divided into 10 bins, each approximately 0.2-0.4  $\mu\text{m}$  in length. Spam protein is specifically localized at the interface between the MRN and lymph space, and in the vicinity of the ciliary dilation (see also panel a). This second site of expression (gray bars) is likely important for the partition of the two cilia in each scolopole, as cilia no longer show the expected separation in *spam* mutants (see for example Fig 2, and data not shown). As a control for the specificity of the antibody and labeling protocol, no label was observed in *spam* null mutants (data not shown). (d-e) Electron micrographs (left) and diagrams (right) of control (d) and *spam* (e) scolopales after 30 min. at 37°C. Note that the MRN invades the scolopale space in the *spam* mutants but not in control flies. Dashed red lines display the tracing of the MRN plasma membrane and dashed gray lines illustrate the location of the cilium. Arrows point at the interface between MRNs and extracellular space. No rupture of the MRN membrane is seen in *spam* mutants following heat treatment. We suggest that the rapid loss of water from the animal's circulatory system (hemolymph) following 30 min at 37°C would increase its osmolarity, leading to an outflow of water from the sensory lymph. The corresponding loss of fluid from the sensory lymph would cause the deformation of the MRN cytosol (in essence by creating a vacuum-like effect in the scolopale space), which if not contained (as in the absence of Spam protein), would then invade the lymph space.



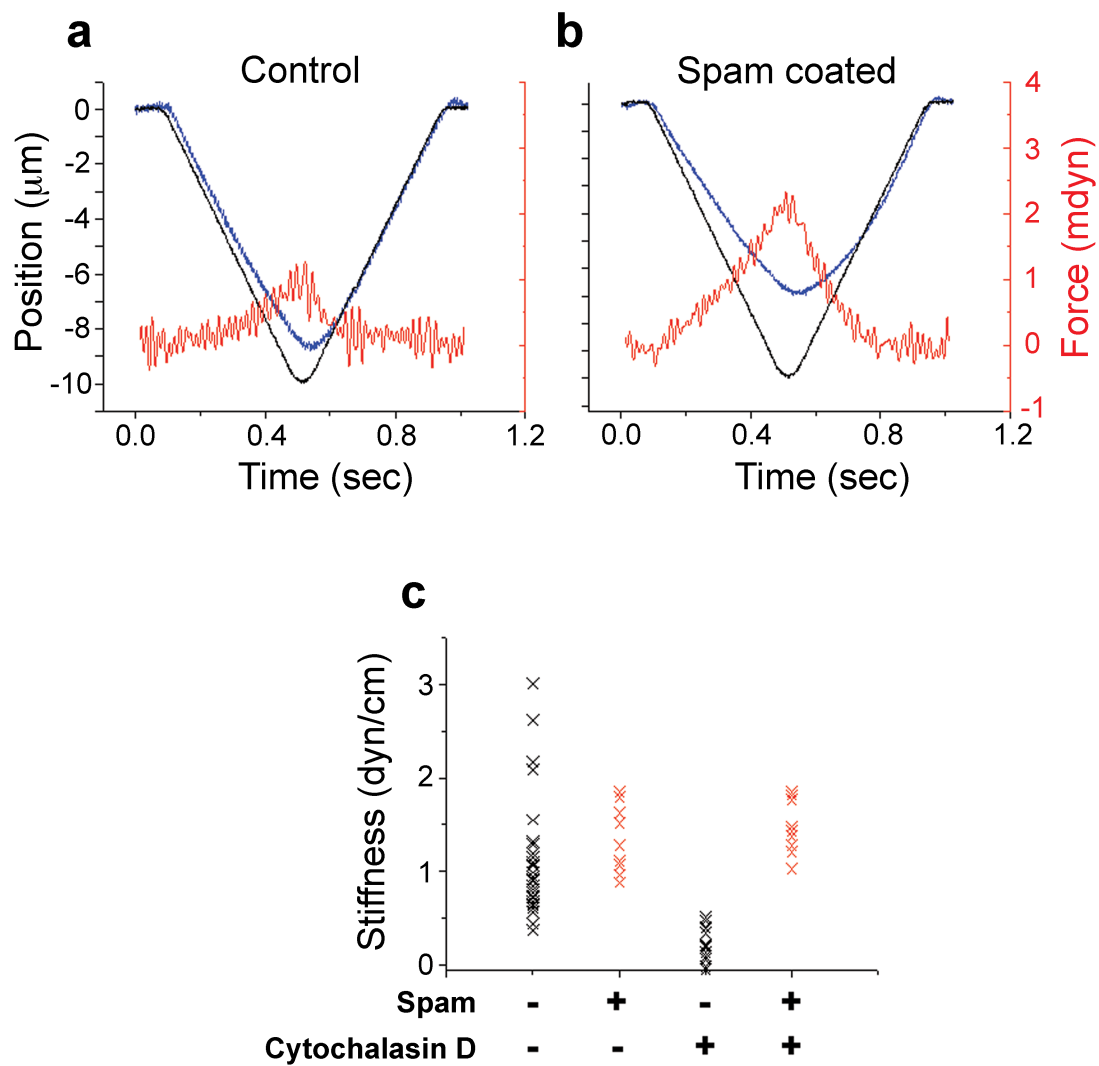


### Trypan blue



#### **Supplementary Figure 5: Survival of tissue culture cells to osmotic shock**

Spam-coated (panel a) and uncoated cells were subjected to sequential osmotic shocks and tested for viability at the end of the experiment using the dye exclusion method. Cells shown in figure 3a-d (upper panel) were placed back into normal culture media after the hyperosmotic shock, and incubated with 0.04% trypan blue. As expected for live cells, the dye is excluded from staining. See figure 3 and main text for additional details on the experiment.



**Supplementary Figure 6: Mechanical impact of spam coating.**

(a) Control or (b) Spam-coated tissue culture cells were subjected to a mechanical indentation assay<sup>14</sup> (see text for details). (c) Stiffness (cell resistance to indentation) was calculated as described<sup>14</sup>. The scatter plots shows stiffness measurements for control and coated-cells with or without cytochalasin D treatment (see also figure 4).

## Supplementary Methods:

**Immunogold electron microscopy.** Fly heads (*cn bw* or *spam* mutants) were fixed in 0.1M phosphate buffer with 4% paraformaldehyde for 2 hrs at 21°C. Samples were cryoprotected in 2.3M sucrose at 4°C overnight and snap-frozen in liquid nitrogen. Cryosections (110nm) of the antennal 2<sup>nd</sup> segment were picked up onto grids and immunolabeled using mAb21A6 monoclonal antibodies<sup>17</sup> (diluted 1:2 to 1:25) and 10nm gold-conjugated goat anti-mouse antibodies (GE Healthcare, Piscataway, NJ). Grids were viewed and photographed using a JEOL 1200EX II transmission electron microscope.

19. T. Avidor-Reiss, A. M. Maer, E. Koundakjian et al., *Cell* 117 (4), 527 (2004).